*17th World Conference on Earthquake Engineering, 17WCEE*

*Sendai, Japan - September 13th to 18th 2020*

# STABILITY ANALYSIS OF MASONRY STRUCTURES UNDER STATIC AND DYNAMIC LOADING USING DISCETE FINITE ELEMENT METHOD

I.H.P. Mamaghani[(1)]

[(1)] *Associate Professor, Department of Civil Engineering, University of North Dakota, iraj.mamaghani@und.edu*

## *Abstract*

Unreinforced masonry structures, consisting of interacting distinct blocks, have been constructed since the earliest days of civilization, are still commonly built in many countries all over the world, and constitute a significant percentage of current structures. Many of these structures are located in seismically active regions and were built before the establishment of any design code requirements for earthquake-resistant construction. Compared with modern structures built of materials with well-understood constitutive laws, the mechanics of masonry structures are still not clearly understood in spite of their long use. The failures and damage reported in recent earthquakes attest to the need for efficient strengthening procedures and therefore an efficient analytical method for analysis of masonry structures. In this paper, first, the discrete finite element method (DFEM) developed by the author for analysis of blocky systems under static and dynamic loading is briefly presented. The DFEM consists of a mechanical model which represents the deformable blocks and contact models that specify the interactions among them. In the DFEM, a visco-elastic constitutive law for linear behavior and a visco-elasto-plastic constitutive law for nonlinear behavior of blocks and contacts are used together with an updated Lagrangian scheme. The DFEM calculates displacements at the joints as well as deformations within the blocks, which can be used to follow the processes of the failure mechanism of masonry structures under static and/or dynamic loadings. Through some illustrative examples, the applicability of the DFEM to the stability analysis of unreinforced masonry structures is investigated and discussed. It has been shown that the DFEM is capable of simulating large displacements of blocky systems, such as open rock slopes, underground openings, tunnels, fault propagation, and fault-structure interaction. It is concluded that the DFEM is a promising method for studying the stability of unreinforced masonry structures.

*Keywords: Unreinforced Masonry Structures;* Discrete Finite Element Method*; Stability Analysis; Contact Element*

## 1. Introduction

Masonry structures, consisting of interacting distinct blocks, have been constructed since the earliest days of civilization, are still commonly built in many countries all over the world, and constitute a significant percentage of current structures. Many of these structures are located in seismically active regions and were built before the establishment of any design code requirements for earthquake-resistant construction. Compared with modern structures built of materials with well-understood constitutive laws, the mechanics of masonry structures are still not clearly understood in spite of their long use. The failures and damage reported in recent earthquakes attest to the need for efficient strengthening procedures and therefore an efficient analytical method for analysis of masonry structures.

The analysis of unreinforced masonry and rock engineering structures excavated in discontinuous rock masses has been receiving particular interest among civil engineers, rock mechanics, and rock engineers. Since rock masses consist of distinct blocks due to geological discontinuities, several techniques have been developed to analyze masses consisting of distinct blocks. A literature review shows that during the last three decades, the limiting equilibrium analysis [1,2] and some numerical analysis methods such as the finite element method (FEM) [3], distinct element method (DEM) [4], and discontinuities deformation analysis (DDA) [5] have been developed for the analysis of problems involving discontinuities in rock mechanics.

The DEM has been used for years in different industries (*e.g.*, mining, civil engineering, and nuclear waste disposal) for the solution of problems involving deformation, damage, fracturing, and stability of fractured rock masses and masonry structures [6-9]. Recently, a number of modeling techniques have been developed to simulate coupled hydro-mechanical problems with the DEM; these methods have been reviewed by author [6,7]. For example, the Universal Distinct Element Code (*UDEC*), developed by Itasca Consulting Group, Inc. [10], utilizes an explicit solution scheme that can model the complex, non-linear behavior of media containing multiple intersecting joint structures. Joint models and properties can be assigned separately to individual discontinuities or sets thereof. The analysis of rock mass stimulation by fluid injection requires analytical tools, such as numerical models based on DEM, which can represent discontinuities explicitly [11]. A similar approach for simulation of fracturing and hydraulic fracturing of rocks is based on the combined finite element method (FEM) and DEM. The formulation of the method and some example applications are found in Rougier *et al.* [12]. In spite of all these techniques, it is difficult to say that a unique technique that guarantees satisfactory results has been developed. Although DEM and DDA can be used for the static and dynamic analysis of discontinuous media, the treatment of rate-dependent behavior of materials in these methods is not realistic. For example, DEM introduces a forced damping to suppress oscillations, while DDA adopts very large time steps so that artificial damping occurs as a result of numerical integration.

In this paper, first, the discrete finite element method (DFEM) developed by the author for analysis of blocky systems under static and dynamic loading [13-17] is briefly presented. The DFEM consists of a mechanical model which represents the deformable blocks and contact models that specify the interactions among them. In the DFEM, a visco-elastic constitutive law for linear behavior and a visco-elasto-plastic constitutive law for nonlinear behavior of blocks and contacts are used together with an updated Lagrangian scheme. The DFEM can handle large block motions within the framework of the finite element method. then, the applicability of the DFEM to the analysis of unreinforced masonry structures such as open rock slopes and pseudo-dynamic analysis of masonry arch structures will be presented and discussed.

## 2. Modeling of Block Contacts

Discontinuum is distinguished from continuum by the existence of discontinuities at contacts between the discrete bodies that comprise the system. The actual geometry of contacts is never smooth and has asperities of varying amplitude and wave length (Aydan et al. 1989). Relative sliding or separation movements in such localized zones present an extremely difficult problem in mechanical modeling and numerical analysis. The most suitable and mechanically sound approach in modeling slope discontinuities is band-type modeling. In this approach contacts between neighboring blocks are considered as bands with a finite thickness. The thickness of the bands is related to the thickness of shear-bands observed in tests or in nature, and the height of asperities along the plane (Aydan et al., 1989). For an idealized contact shown in Fig. 1, the average normal and shear stresses and strains are defined as follows:

$$\sigma_n = \frac{F_n}{A} \tag{1}$$

$$\varepsilon_n = \frac{\delta_n}{A} \tag{2}$$

$$\tau_s = \frac{F_s}{A} \tag{3}$$

$$\gamma_s = \frac{F_s}{h} \tag{4}$$

where, $A$ and $h$ are the area and the thickness of the band; $F_n$ and $F_s$ stand for the normal and tangential forces; and $\delta_n$ and $\delta_s$ denote the normal and tangential deformations, respectively (Fig. 1). Furthermore, it is also possible to define the average strain rates $\dot{\varepsilon}_n$ and $\dot{\gamma}_n$. As a result, this model also enables one to define stress-strain rate dependent responses, objectively. The problem is, then, to select a constitutive model such as an elastic, elasto-plastic or elasto-visco-plastic type constitutive law which is appropriate for modeling the mechanical behavior of contacts between neighboring blocks.

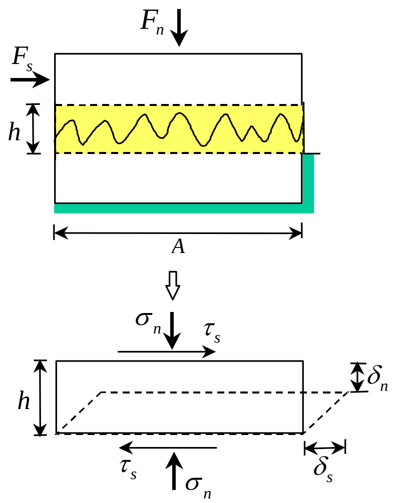


Fig. 1 : Mechanical model of a contact as a band

## 3. Discrete Finite Element Method (DFEM)

The developed DFEM, in assessing the stability of rock block systems such as rock slopes, is based on the finite element method. It consists of a mechanical model to represent the deformable blocks and contact models that defines the interaction among them. The deformation of blocks is assumed to be small unless they are allowed to rupture. Small displacement theory is applied to the deformable blocks while blocks can take finite displacement. The large deformation of blocky systems is associated with separation, translation and rotation of blocks. Blocks are polygons with an arbitrary number of sides, which are in contact with the neighboring blocks, and are idealized as a single element or multiple finite elements. Block contacts are represented by contact elements.

### 3.1 Mechanical Modeling

The general equation of motion is given by

$$\nabla \cdot \boldsymbol{\sigma} + \boldsymbol{b} = \rho \ddot{\boldsymbol{u}} \tag{5}$$

where $\boldsymbol{\sigma}$, $\boldsymbol{b}$, ρ, and $\ddot{\boldsymbol{u}}$ are stress tensor, body force, mass density, and acceleration, respectively. The following presentation is restricted to the framework of the small-strain theory. The strain $\boldsymbol{\varepsilon}$-displacement $\boldsymbol{u}$ relations are represented by



 

$$\boldsymbol{\varepsilon} = \frac{1}{2}[\nabla \boldsymbol{u} + (\nabla \boldsymbol{u})^T] \tag{6}$$

The strain rate $\dot{\boldsymbol{\varepsilon}}$ -velocity $\boldsymbol{v}$ relations are given by

$$\dot{\boldsymbol{\varepsilon}} = \frac{1}{2}[\nabla \boldsymbol{v} + (\nabla \boldsymbol{v})^T] \tag{7}$$

where $\boldsymbol{v} = \dot{\boldsymbol{u}}$. The following constitutive relationship among stresses and strains and strain rates holds:

$$\boldsymbol{\sigma} = \boldsymbol{D}_e \boldsymbol{\varepsilon} + \boldsymbol{D}_v \dot{\boldsymbol{\varepsilon}} \tag{8}$$

where $\boldsymbol{D}_e$ and $\boldsymbol{D}_v$ are elasticity and viscosity tensors (Mamaghani, 1993), respectively. However, they can be replaced by elasto-plastic and visco-plastic tensors, if necessary. This type of constitutive law allows for the modelling of intact blocks as well as contacts, interfaces, or rock discontinuities. The boundary conditions are $\boldsymbol{u} = \hat{\boldsymbol{u}}$ on $\Gamma_u$ and $\hat{\boldsymbol{t}} = \boldsymbol{\sigma} \cdot \boldsymbol{n}$ on $\Gamma_t$, where $\hat{\boldsymbol{u}}$ is the displacement on boundary $\Gamma_u$ and $\hat{\boldsymbol{t}}$ is the surface traction in the *n* direction on boundary $\Gamma_t$. The initial conditions are $\boldsymbol{u_o}$ and $\hat{\boldsymbol{u}}_{\boldsymbol{o}}$ at $t = 0$.

3.2 Finite Element Modeling

In the following discussion, the finite element form of the equation of motion is derived. Taking a variation on $\delta \boldsymbol{u}$, the integral form of Eq. (5) can be written as

$$\int_{\Omega} (\nabla \cdot \boldsymbol{\sigma}) \cdot \delta \boldsymbol{u} d\Omega + \int_{\Omega} \boldsymbol{b} \cdot \delta \boldsymbol{u} d\Omega = \int_{\Omega} \rho \ddot{\boldsymbol{u}} \cdot \delta \boldsymbol{u} d\Omega \tag{9}$$

With the use of the Gauss divergence theorem and the boundary conditions, the weak form of the governing equation takes the following form:

$$\int_{\Gamma_t} \hat{\boldsymbol{t}} \cdot \delta \boldsymbol{u} d\Gamma + \int_{\Omega} \boldsymbol{b} \cdot \delta \boldsymbol{u} d\Omega = \int_{\Omega} \boldsymbol{\sigma} \cdot (\nabla \delta \boldsymbol{u}) d\Omega + \int_{\Omega} \rho \ddot{\boldsymbol{u}} \cdot \delta \boldsymbol{u} d\Omega \tag{10}$$

Eq. (10) is discretized in the space domain by assuming displacements are approximated by the following expression:

$$\boldsymbol{u} = \boldsymbol{N} \boldsymbol{U}(t) \tag{11}$$

where $\boldsymbol{N}$ is the shape function. Using the approximate form and the constitutive law, the following expressions, in condensed form, are obtained for a typical finite element (Mamaghani, 1993; Mamaghani *et al*., 1999):

$$\boldsymbol{M}\ddot{\boldsymbol{U}} + \boldsymbol{C}\dot{\boldsymbol{U}} + \boldsymbol{K}\boldsymbol{U} = \boldsymbol{F} \tag{12}$$

*where* **F** *is the force vector and* M, C, *and* K, *are the mass, damping, and stiffness matrices, respectively. They are defined as follows (Mamaghani, 1993):*

$$\boldsymbol{M} = \int_{\Omega_e} \rho \boldsymbol{N}^{\boldsymbol{T}} \boldsymbol{N} d\Omega \tag{13}$$

$$\boldsymbol{C} = \int_{\Omega_e} \boldsymbol{B}^{\boldsymbol{T}} \boldsymbol{D}_V \boldsymbol{B} d\Omega \tag{14}$$



 

$$\boldsymbol{K} = \int_{\Omega_e} \boldsymbol{B}^T \boldsymbol{D}_e \boldsymbol{B} d\Omega \tag{15}$$

$$\boldsymbol{F} = \int_{\Omega_e} \boldsymbol{N}^T \boldsymbol{b} d\Omega + \int_{\Gamma_{te}} \bar{\boldsymbol{N}}^T \boldsymbol{t} d\Gamma \tag{16}$$

### 3.3 Modeling of Contacts

The contact element is used to model contacts of blocks in rock slope discontinuities. Let's consider a two-nodded element $l, m$ in two-dimensional space and take two coordinate systems $oxy$ and $o'x'y'$ as shown in Fig. 2. Assuming that, the strain component $\varepsilon_{y'y'}$ is negligible, the remaining strain components take the following forms:

$$\varepsilon_{x'x'} = \frac{\partial u'}{\partial x'} \tag{17}$$

$$\gamma_{x'y'} = \frac{\partial v'}{\partial x'} \tag{18}$$

Let us assume that the shape functions are linear such that:

$$N_l = 0.5(1-\xi) \tag{19}$$

$$N_m = 0.5(1+\xi) \tag{20}$$

where $\xi = (-2x' + x'_l + x'_m)/L,\ L = (x'_l - x'_m)$ . Then, the relation between the strains and nodal displacements becomes:

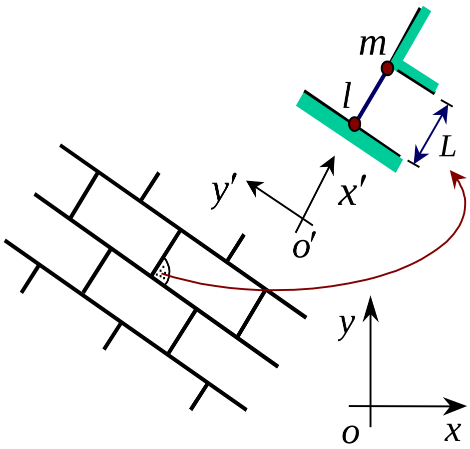

Fig. 2: Modeling blocks contact

$$\begin{Bmatrix} \varepsilon_{x'x'} \\ \gamma_{x'y'} \end{Bmatrix} = \frac{1}{L} \begin{bmatrix} -1 & 0 & 1 & 0 \\ 0 & -1 & 0 & 1 \end{bmatrix} \begin{Bmatrix} U'_l \\ V'_l \\ U'_m \\ V'_m \end{Bmatrix} \tag{21}$$



 

Thus, the stiffness matrix of contact element in the local coordinate system is explicitly obtained as:

$$\boldsymbol{K}' = \begin{bmatrix} k'_n & 0 & -k'_n & 0 \\ 0 & k'_s & 0 & -k'_s \\ -k'_n & 0 & k'_n & 0 \\ 0 & -k'_s & 0 & k'_s \end{bmatrix} \tag{22}$$

$$k'_n = E_n.\frac{A_c}{x'_m - x'_l} \tag{23}$$

$$k'_s = G_s.\frac{A_c}{x'_m - x'_l} \tag{24}$$

where $A_c$ is the contact area, $E_n$ and $G_s$ are normal and shear elastic moduli of discontinuity, respectively.

The stiffness matrix in the local coordinate system is then transformed to the stiffness matrix in the global coordinate system by the following relationship:

$$\boldsymbol{K} = \boldsymbol{T}^T \boldsymbol{K}' \boldsymbol{T} \tag{25}$$

where,

$$\boldsymbol{T} = \begin{bmatrix} cos\theta & \sin\theta & 0 & 0 \\ -\sin\theta & \cos\theta & 0 & 0 \\ 0 & 0 & cos\theta & \sin\theta \\ 0 & 0 & -\sin\theta & \cos\theta \end{bmatrix} \tag{26}$$

$$\theta = tan^{-1}\left(\frac{y_m - y_l}{x'_m - x'_l}\right) \tag{27}$$

The viscosity (damping) matrix of a contact element in the local coordinate system can also be obtained in a similar manner as given below:

$$\boldsymbol{C}' = \begin{bmatrix} c'_n & 0 & -c'_n & 0 \\ 0 & c'_s & 0 & -c'_s \\ -c'_n & 0 & c'_n & 0 \\ 0 & -c'_s & 0 & c'_s \end{bmatrix} \tag{28}$$

$$c'_n = E^*_n.\frac{A_c}{x'_m - x'_l} \tag{29}$$

$$c'_s = G^*_s.\frac{A_c}{x'_m - x'_l} \tag{30}$$

where, $E^*_n$ and $G^*_s$ are normal and shear viscosity moduli of the discontinuity, respectively. In the above equations, the values of coefficients in the stiffness and viscosity matrices, as well as the value of $\theta$ are affected by updating geometrical changes of blocks and contacts.



 

It is worth noting that on the basis of simplification of the finite element modeling of block contacts, using the small strain theory for modeling of the large deformation, a small error is always present in the computed strains of contacts. Nevertheless, such an error is quite negligible as the geometry of the block system is incrementally updated, which takes into account the effect of higher order terms in the definition of finite strain tensor.

## 4. Numerical Results and Discussions

In this section, some typical numerical results of slope stability obtained by the DFEM will be presented and discussed. In the numerical study, when the inertia term is considered, contacts and blocks are assumed to behave as an elasto-visco-plastic material or a visco-elastic material. On the other hand, if the inertia term is omitted, the behavior of contacts and blocks is assumed to be elasto-plastic or elastic. In all analyses reported herein, tensile strength of contact elements was assumed to be zero. Mohr-Coulomb yield criterion was implemented in the present codes. Nevertheless, one can easily implement any yield criterion, which is appropriate for the plastic or visco-plastic behavior. Contact area $A_c$ was assumed to be half the area of the side of a block to which the contact element was attached. The thickness of the bands was taken as twice the weighted asperity height. Taking into account the results reported by Aydan et al. (1989), the thickness of the bands was selected as 10 mm. The secant stiffness method together with updated Lagrangian Scheme was employed to deal with non-linear behavior. The constant strain triangular element with two degrees of freedoms at each node, formed by properly joining the corners and contact nodes of an individual block, was adopted for finite element meshing of the blocks (Mamaghani, 1993). However, it must be noted that the method is not restricted to the use of such elements and one can easily implement finite elements of chosen nodes.

The analysis is a pseudo time stepping incremental procedure. First the initial configuration of the structural system, boundary conditions and material properties are input. Then iterations are carried out by forming the global stiffness matrix and solving equilibrium equations of the system. Later the strains and stresses of elements are computed. The no-tension condition and Mohr-Coulomb's yield criterion are checked and the excess forces at contacts are applied to the updated configuration as the penalty load in the subsequent iteration until the norm of excess force vector converges to a very small value of convergence tolerance. The computation is terminated when a stable configuration is achieved or the global stiffness matrix becomes ill-conditioned as single or multiple blocks tends to move without any interaction with each other corresponding to the failure of the system. The details of the numerical algorithm and computational procedure are given in the work by the author [13].

### 4.1 Stability of One Block on an Incline

A very simple, yet meaningful problem analyzed by the DFEM is the stability of one block on an incline. The theoretical kinematic conditions for sliding and toppling of one block on an incline, under gravity, have been given in a chart by Hoek and Bray (1977), hereafter referred to as H-B chart. The H-B chart with the friction angle between the block and the incline $\phi = 20^{\circ}$ is shown in Fig. 3. In the H-B chart, four modes of behavior, namely, (a) stability, (b) sliding without toppling, (c) sliding and toppling, and (d) toppling without sliding are delineated by four boundaries I, II, III and IV. The DFEM is applied to study the stability of one block on an incline, and the results are compared with those predicted by the H-B chart.

In the numerical analysis, the assumed material properties of intact blocks are: Lame's constants $\lambda = 56GPa$ and $\mu = 21GPa$, and unit weight $\rho = 25kN/m^3$. The properties of contacts are assumed as: normal stiffness, $E_n = 50GPa$, and shear stiffness, $G_S = 0.5GPa$. For a methodical comparison, the slope angle, $\alpha$, and the aspect ratio of the block, $\gamma = \arctan(b/d)$, ($b$ = breadth; $d$ = height of the block, Fig. 3) were varied systematically, while the friction angle, $\phi$, was fixed at $20^\circ$. Different symbols representing different modes of behavior obtained by the DFEM are plotted on the H-B chart as shown in Fig. 3. As can be seen from these plots, the results by the proposed method are in complete agreement with the theoretical results. Since the validity of the theoretical solutions are also validated by experiments [1, 2], it can be concluded that the DFEM is a promising method for studying the mechanics of blocky media.

### 4.2 Dynamic Stability

The dynamic stability of square and rectangular blocks on a plane with an inclination of $30^\circ$ was analyzed by the DFEM. The rectangular block was assumed to have a height to breadth ratio $h/b = 1/3$. The assumed material properties of the intact rock blocks and mechanical properties of the contact elements used in numerical analyses are given in Table 1. In the table $\lambda$, $\mu$, $\lambda^*$ and $\mu^*$ stand for the elastic and viscous

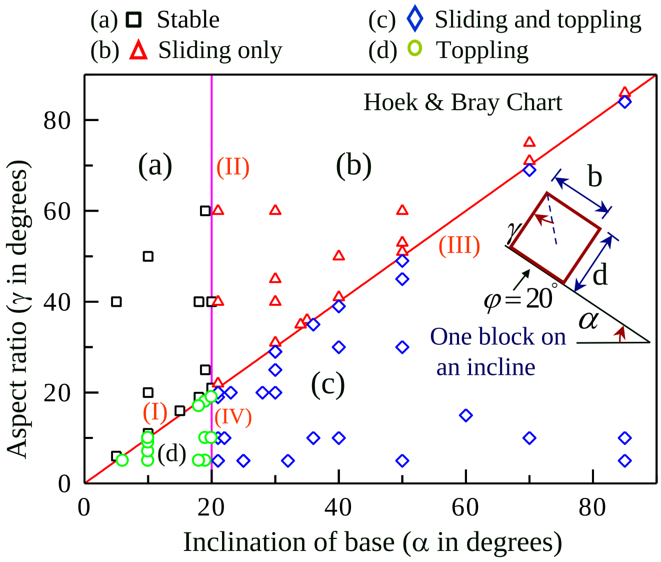


Fig. 3: Kinematic conditions of one block on an incline
(DFEM versus theoretical results)

Lame's constants, respectively. $\rho$ denotes the unit weight of the blocks. $E_n$, $E_s$, $E_n^*$ and $G_s^*$ stand for the elastic and viscous normal and shear modulus of the contact, respectively. The friction angles for square and rectangular blocks are $\phi = 25^\circ$ and $\phi = 35^\circ$, respectively. Fig. 4 shows computed configurations of the square block of size $4m \times 4m$ and a rectangular block of size $12m \times 4m$. The square block slides on the incline (time step $\Delta t = 0.04\,\text{sec}$) while the rectangular block topples (time step $\Delta t = 0.01\,\text{sec}$). These predictions are consistent with the kinematic conditions for the stability of a single block in the previous example as well as with the experimental results reported by Aydan et al. (1989) [1]. It should, however, be noted that the discretization of the domain, mechanical properties of blocks and contacts and time steps may cause superficial oscillations and numerical instability.



 

It is worth noting that any hyperbolic type equation system; (i.e., Equation 2), requires a certain kind of damping (viscosity) to attain a stationary solution, which requires information on the viscous characteristics of rocks and discontinuities. Since time-dependent characteristics of discontinuities and intact

Table 1: Properties of intact rock and contacts

| Properties of Blocks | | | | | Properties of Contacts | | | | | | |
|---|---|---|---|---|---|---|---|---|---|---|---|
| $\lambda$ | $\mu$ | $\lambda^*$ | $\mu^*$ | $\gamma$ | $E_n$ | $G_s$ | $E_n^*$ | $G_s^*$ | $c$ | $\sigma_t$ | $\varphi$ |
| $MPa$ | $MPa$ | $MPa \cdot s$ | $MPa \cdot s$ | $kN/m^3$ | $MPa$ | $MPa$ | $MPa \cdot s$ | $MPa \cdot s$ | $MPa$ | $MPa$ | $(^\circ)$ |
| 10 | 10 | 5 | 5 | 25 | 0.1 | 0.1 | 0.05 | 0.05 | 0 | 0 | (25) 35 |

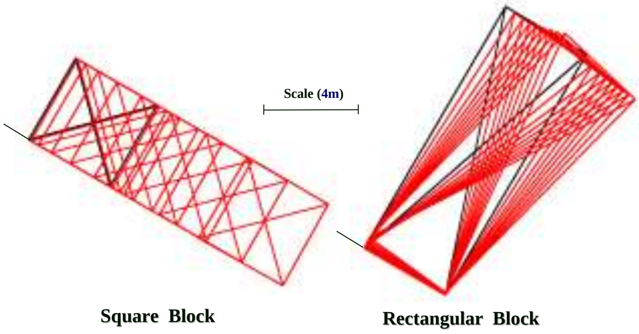


Fig. 4: Dynamic stability of a block on incline

rocks are less studied and experimental data are still limited, the inertia term is neglected in the computations reported hereafter. Also, hereafter, in all computations the loading was assumed to be resulting from the gravitational pull.

### 4.3 Pseudo-dynamic analysis of masonry arch structures

This section is concerned with the application of DFEM to the dynamic analysis of masonry arch structures. In the analysis, the foundation of the structures was subjected to two types of lateral acceleration waves: Acc. No. 1 with a large period:

$$Acc = 0.8te^{-0.5t}\sin(t)\times 981 \tag{1}$$

and Acc. No. 2 with a small period:

$$Acc = 0.8te^{-0.5t}\sin(3t)\times 981 \tag{2}$$

for which $t$ = time and $Acc$ = lateral acceleration in $gal$, as shown in Fig. 5.

The assumed accelerations are used to check the response of analyzed masonry structures by DFEM under two different waveforms. The material and mechanical properties of blocks, foundations, and contacts for the analyzed masonry arch are given in Table 2, where $\lambda$, $\mu$, $\lambda^*$, and $\mu^*$ indicate the elastic and viscous Lame's constants. $\rho$ denotes the unit weight of the rock mass. $E_n$, $G_s$, $E_n^*$, and $G_s^*$ indicate the elastic and viscous normal and shear modulus of the contact. $h$ and φ indicate band width of contact elements and friction angle, respectively. In all examples, the time step was chosen as 0.2 sec. In the following dynamic analysis of the three masonry structures, in the plots of the deformed configurations, the displacement in the deformed configurations is amplified by 50 times to make the deformed configuration (mode of failure) more visible from the initial configuration.



 

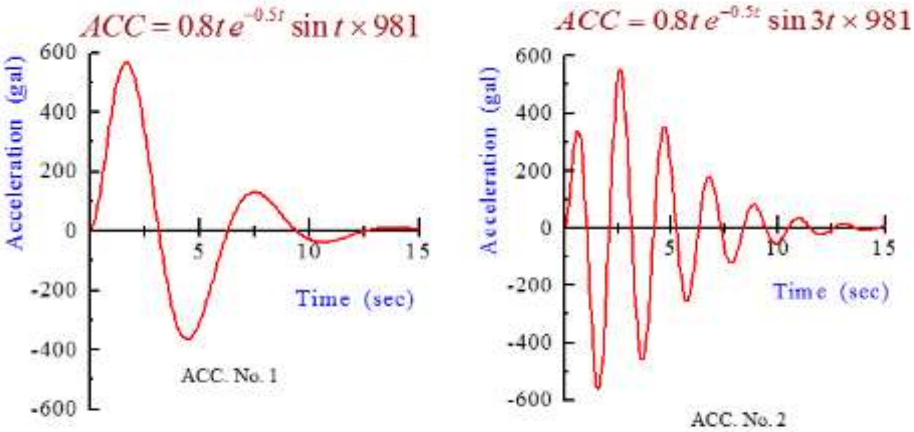

Fig. 5: Imposed lateral acceleration waves on foundation.

Table 2: Material properties of rock blocks and contacts for the analyzed masonry arch.

| ***Structures*** | ***Properties of Blocks*** | | | | | ***Properties of Contacts*** | | | | | |
|---|---|---|---|---|---|---|---|---|---|---|---|
| | ***λ*** | ***μ*** | ***λ**** | ***μ**** | ***ρ*** | $E_n$ | $G_s$ | $E_n^*$ | $G_s^*$ | ***h*** | ***φ*** |
| | ***MPa*** | ***MPa*** | ***MPa*** | ***MPa*** | ***kN/m³*** | ***MPa*** | ***MPa*** | ***MPa.s*** | ***MPa.s*** | ***mm*** | ***( ° )*** |
| Arch, Tower | 30 | 30 | 30 | 30 | 25 | 50 | 25 | 5 | 2.5 | 5 | 35 |

Figs. 6a, 6c, and 6d show the initial and deformed configurations of a masonry arch at the 23rd time step (4.6 seconds) and 50th time step (10 seconds) subjected to Acc. No. 1 and Acc. No. 2, respectively. Fig. 6c shows that the arch is sliding at the base at the 23rd time step under Acc. No. 1, and the crown blocks of the arch start to fall apart while the side columns are still stable. Fig. 6c shows that, under Acc. No. 1 at the 50th time step, the arching action disappears and the crown blocks fall apart. The columns slide relative to the base, and they tend to topple in two opposite directions. The blocks tend to separate within the side columns (Fig. 6c).

Figure 6d shows that, under Acc. No. 2 at the 23rd time step, there is no sliding at the base of the arch, while the crown blocks are separated and tend to fall apart. At the 23rd time step, the side columns of the arch exhibit relatively stable behavior under Acc. No. 2 as compared with the Acc. No. 1 (Figs. 6c and 6d). However, under Acc. No. 2 at the 50th time step (10 seconds), the side columns of the arch slide at the base, and the arching action disappears while the blocks start to fall apart. As expected, the toppling (failure) modes of the side columns of the arch differ depending on the nature of the imposed form of acceleration waves, as shown in Figs. 6c and 6d for the 50th time step.

Fig. 6b shows the displacement responses with time of a nodal point at the top most-right corner of the arch corresponding to Acc. No. 1 and Acc. No. 2. The results in Fig. 6b indicate that, as expected, the displacement of the side column of the arch with time is much severe under Acc. No. 1 as compared with Acc. No. 2, especially in the early stage of loading. Fig. 6c and 6d show that, under both of the imposed acceleration waves, the reaction of the toppled columns forces the crown block to move upward. This is because of the geometrically symmetric configuration of the structure and outward inclination of the crown block contact interfaces at the center of symmetry (Fig. 6a). As can be observed by examining the displacement response curves in Fig. 6b, the real value of the displacement is very small as compared with the dimension of the crown block.



 

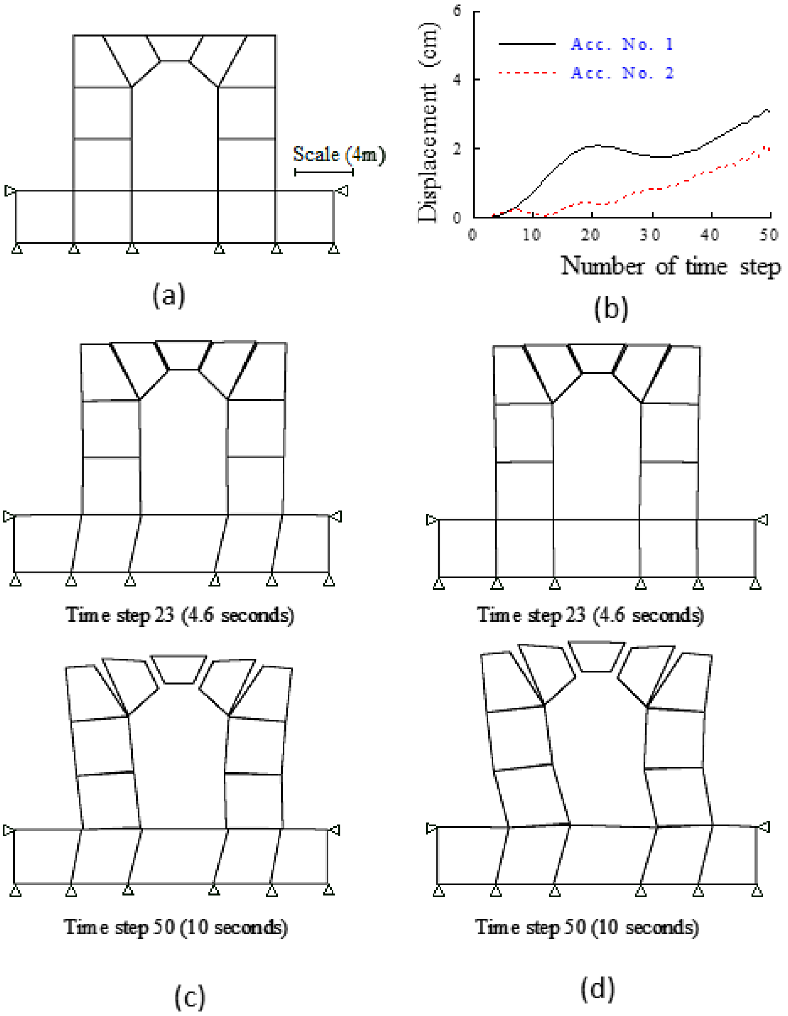


Fig. 6: Initial and deformed configurations and displacement response with time of the arch: (a) Initial configuration, (b) Displacement response with time at the top right corner, (c) Deformed configuration under acceleration No. 1, (d) Deformed configuration under acceleration No. 2

## 5. Conclusions

This paper was concerned with stability analysis of slopes, which are composed of a finite number of distinct, interacting blocks that have a length scale relatively comparable with the slope of interest, using the discrete finite element method (DFEM) recently developed by the authors. The DFEM is based on the principles of the finite element method incorporating contact elements. It considers blocks as sub-domains and represents them by solid elements. Contact elements are used to model the block interactions such as sliding or separation. The DFEM calculates displacements at the joints as well as deformation within the blocks, which can be used to follow the processes of the failure mechanism of slopes under static as well as dynamic loading. Through some typical illustrative examples, the applicability of the DFEM to stability analysis of rock slopes were investigated and discussed. It has been shown that the DFEM is capable of simulating large displacement of blocky systems, such as open rock slopes and underground openings. It was found that the DFEM is a promising method for studying stability of blocky slopes. However, the hyperbolic scheme of the DFEM is still in its formative phase for which both experiments on viscous characteristics of blocks and contacts as well as a numerically stable time-discretization scheme are felt to be necessary.



 

## 6. References

[1] Aydan Ö, Shimizu Y and Ichikawa Y (1989): The effective failure modes and stability of slopes in rock mass with two discontinuity sets. *Rock Mechanics and Rock Engineering*, Vol. 22(3), pp. 163-188.

[2] Hoek E and Bray JW (1977): Rock Slope Engineering. T*he Institution of Mining and Metallurgy*, Revised Second Edition, London.

[3] Goodman RE, Taylor R and Brekke TL (1968): A model for the mechanics of jointed rock. *J. of Soil Mechs. and Found. Eng. Div.*, ASCE, SM3, Vol. 94(3), pp. 637-659.

[4] Cundall PA (1971): A computer model for simulating progressive, large-scale movements in blocky rock systems. *Proc. Int. Symp. on Rock Fracture*, II-8, Nancy, France.

[5] Shi GH (1988): Discontinuous deformation analysis: a new numerical model for the statics and dynamics of block system. *PhD Thesis*. Dept. of Civil Engineering, University of California, Berkeley.

[6] Mamaghani IHP (2016): Chapter 15, Discrete Finite Element Method for Analysis of Masonry Structures, *Computational Modeling of Masonry Structures Using the Discrete Element Method*, Editors: Sarhosis, V., Bagi, K., Lemos, J.V., Milani, G., ISBN13: 9781522502319 & EISBN13: 9781522502326, pp. 393-415.

[7] Mamaghani IHP (2016): Chapter 17, Application of Discrete Finite Element Method for Analysis of Unreinforced Masonry Structures, *Computational Modeling of Masonry Structures Using the Discrete Element Method*, Editors: Sarhosis, V., Bagi, K., Lemos, J.V., Milani, G., ISBN13: 9781522502319 & EISBN13: 9781522502326, pp. 440-458.

[8] Brandenberg SJ, Manzari M (2018): Geotechnical Earthquake Engineering and Soil Dynamics V: Slope Stability and Landslides, Laboratory Testing, and In-Situ Testing, *ASCE Geotechnical Special Publications (GSP) GSP 293*, ISBN: 9780784481486.

[9] Abbasi B, Russell D, and Taghavi R (2013): FLAC3D mesh and zone quality," Continuum and Distinct Element Numerical Modeling in Geomechanics, *Zhu, Detournay, Hart, and Nelson (eds.),* Paper: 11-02, Itasca International Inc., Minneapolis, 12 pages, ISBN 978-0-9767577-3-3.

[10] Itasca Consulting Group Inc (2014): UDEC Version 6., Distinict-Element Modeling of jointed and Blocky Material in 2D, http://www.itascacg.com/software/udec.

[11] Damjanac, B., Detournay, C. Cundall, P.A. (2015). Application of particle and lattice codes to simulation of hydraulic fracturing, http://www.itascacg.com/application-of-particle-and-lattice-codes-to-simulation-of-hydraulic-fracturing

[12] Rougier E, Knight EE, Munjiza A (2012). Fluid driven rock deformation via the combined FEM/DEM methodology. In: American rock mechanics association 46thUS rockmechanics/ geomechanics symposium held in Chicago, 24–27 June 2012, number ARMA12- 516.

[13] Mamaghani, I.H.P. (1993). "Numerical analysis for stability of a system of rock blocks". *Master Thesis.* Department of Civil Engineering, Nagoya University, Nagoya, Japan.

[14] Mamaghani IHP, Baba S, Aydan Ö and Shimizu Y (1994): Discrete finite element method for blocky systems. *Proc. of the Eighth Int. Conf. on Computer Methods and Advances in Geomechanics (IACMAG),* Morgantown, USA, Vol. 1, pp. 843-850.

[15] Mamaghani IHP, Aydan Ö and Kajikawa Y (1999): Analysis of masonry structures under static and dynamic loading by discrete finite element method. *Journal of Structural Mechanics and Earthquake Engineering*. Japan Society of Civil Engineers, JSCE, No. 626/I-48, pp. 1-12.

[16] Mamaghani IHP (2006): Analysis of Masonry Bridges: Discrete Finite Element Method. *Journal of Transportation Research Board,* Washington D.C., Issue Number 1976, pp. 13-19.

[17] Mamaghani, I.H.P (2015) Discrete Finite Element Method Application for Analysis of Unreinforced Masonry Underground Structures, *TRB annual meeting*, Paper ID: 15-4336.



 